Cubic-to-tetragonal structural phase transition in $Rb_{1-x}Cs_xCaF_3$ solid solutions: Thermal expansion and EPR studies

F. Lahoz, B. Villacampa, R. Alcalá, C. Marquina, and M. R. Ibarra
Instituto de Ciencia de Materiales de Aragón and Departamento de Física de la Materia Condensada, Universidad de Zaragoza-CSIC, Facultad de Ciencias, 50009 Zaragoza, Spain
(Received 16 September 1996)

The influence of crystal mixing on the structural phase transitions in $Rb_{1-x}Cs_xCaF_3$ ($0<x<1$) fluoroperovskite crystals has been studied by thermal expansion and EPR measurements of Ni^{2+} and Ni^{3+} paramagnetic probes. A cubic-to-tetragonal phase transition has been detected in crystals with $x=0$, 0.1, 0.21, 0.27, and 0.35. The critical temperature and the tetragonal distortion decrease as x increases. No transition was observed for $x \geq 0.44$. This transition shows a weak first-order component in the $x=0$ and 0.1 samples, which is progressively smeared out for $x>0.1$, indicating a spatial distribution of the critical temperature in those crystals with high ionic substitution rate. In $RbCaF_3$, another structural phase transition was observed at 20 K with a thermal hysteresis between 20 and 40 K. This transition has not been found in any of the mixed crystals. [S0163-1829(97)05313-7]

INTRODUCTION

Structural phase transitions (SPT) in cubic fluoroperovskites (AMF_3) are strongly dependent on the stabilizing role of the cations. Different studies have been reported on the SPT's in mixed fluoroperovskites in which a partial substitution of either the monovalent (A) or the divalent (M) cations has taken place. The most complete set of studies has been performed in mixed crystals based on $KMnF_3$,[1–6] although the rate of substituted cations was less than 30% in all the cases and less than 10% in most of them.

$KMnF_3$ shows three SPT's at 186 K, 88 K, and 82 K (Ref. 4) characterized by the following transformations: cubic→tetragonal→orthorhombic I→orthorhombic II. All of these transitions are related to different rotations of the fluorine octahedra around the ⟨100⟩ cubic directions. In the mixed crystals, it has been observed that the transition temperatures increase when a bigger divalent cation such as Ca^{2+} is substituted for Mn^{2+} (Refs. 2 and 4), and decrease when a smaller ion such as Mg^{2+} is substituted for Mn^{2+}. An opposite behavior is observed for monovalent cations. In this case, the transition temperatures decrease when a bigger ion such as Rb^+ is substituted for K^+ (Ref. 1) and increase when a smaller ion such as Na^+ is substituted for K^+.[2,3] Besides, changes in the nature of the transitions have been observed in some of the mixed crystals as compared with the pure ones.[2–4,6]

In some recent papers[7–9] Buzaré and co-workers have reported several studies of the SPT's in $Rb_{1-x}K_xCaF_3$ crystals with $x<0.2$. $RbCaF_3$ has the cubic perovskite structure at room temperature (RT) and undergoes two structural phase transitions.[10,11] a cubic to tetragonal one at about 195 K and a tetragonal to orthorhombic one with a thermal hysteresis between 40 and 20 K. The crystal structures of the different phases in $RbCaF_3$ coincide with those of the cubic, tetragonal, and orthorhombic II phases in $KMnF_3$. The 195 K SPT has a second-order character with a weak first-order component while the low-temperature SPT is first order. It has been found that the partial substitution of Rb^+ by K^+ produces an increase of both transition temperatures, in agreement with the results in the $KMnF_3$ family.

The stability of the cubic perovksite structure in different pure and mixed crystals has been discussed by several authors.[12,13] Simple approaches to this problem allow us to relate that stability to the radii of the ions present in the crystals and their concentrations. A rough estimation of the cubic-to-tetragonal transition temperature for different crystal compositions[2,9] has been achieved using these approaches. However, the data available up to now correspond to low rates of substituted cations. Moreover, in the case of mixed crystals based on $RbCaF_3$, only the effects of the substitution of Rb^+ by a smaller ion (K^+), have been studied, and the possible influence of this substitution on the nature of the transitions has not been reported. Because of this, it seems interesting to extend the studies of SPT's to other mixed crystals based on $RbCaF_3$ and with a bigger range of substitution rates.

In this paper we present a study of the cubic-to-tetragonal SPT in $Rb_{1-x}Cs_xCaF_3$ crystals with $0 \leq x \leq 1$. Linear thermal expansion (LTE) has been used to determine the transition temperatures, the presence of the first-order component of this transition, and to estimate the critical exponent β. These β values agree with those obtained by EPR measurements of Ni^{2+} ions in the $x=0$ and $x=0.1$ samples. The influence of the mixture on the distortion of the tetragonal Ni^{3+} centers has also been investigated by EPR.

We aim in this work to explore the changes in the critical temperature of the cubic-to-tetragonal SPT in $RbCaF_3$ upon substitution of Rb^+ by a bigger cation such as Cs^+. In order to test the validity of the methods proposed to estimate the transition temperatures in mixed crystals, we have extended the range of x values up to $x=1$. The possible influence of the substitution on the tetragonal distortion and on the nature of this SPT has also been investigated.

EXPERIMENTAL DETAILS

The pure and mixed $Rb_{1-x}Cs_xCaF_3$ crystals ($0 \leq x \leq 1$)) investigated in this work have been grown by the Bridgman

TABLE I. Analysis of the crystal composition x performed by atomic emission spectroscopy in the crystal family $Rb_{1-x}Cs_xCaF_3$.

Nominal composition (x)	0	0.1	0.2	0.3	0.4	0.5	0.7	0.9	1
Analyzed composition (x)	0	0.1	0.21	0.27	0.35	0.44	0.67	0.9	1

technique. A small NiF_2 concentration (about 1 mol % in the starting materials) was added to the mixtures in order to introduce Ni^{2+} impurities, which were subsequently transformed to Ni^{3+} by x-irradiation at RT. Nickel segregation makes its content in the crystals much lower than in the starting material. It has been checked that neither nickel impurities nor radiation-induced defects influence the transition temperature in pure $RbCaF_3$ within the experimental accuracy.

X-ray diffraction measurements were performed in a D-max Rigaku equipment, with a rotating cathode. The diffractometer works at 45 kV and 80 mA. The $K\alpha$ lines of the Cu cathode were selected with a graphite monochromator.

Thermal expansion measurements were carried out using the strain gauge technique. Two gauges (Micromeasurements model SK-350), one glued on the sample and a dummy one glued on a silica disk, were placed in compensating arms of a modified Wheastone bridge. The gauge in the sample was along one of the $\langle 100 \rangle$ directions of the cubic crystals. A low drift dc amplifier was used to detect the unbalance produced by the sample thermal expansion, $\Delta l(T)/l_0$, with an accuracy of 10^{-6}. $\Delta l(T)$ is the change of the crystal length between RT and the temperature T and l_0 the initial length (in our case the length at RT). The temperature was varied between 300 and 10 K, by using a liquid-helium continuous flow cryostat.

EPR measurements were taken in a computer-controlled Varian E-112 spectrometer working in the x band. Low temperatures were achieved using a liquid-helium flow cryostat. Magnetic-field values were measured with a gaussmeter and the signal of diphenylpicrylhydrazyl at $g=2.0037$ was used to determine the microwave frequency.

EXPERIMENTAL RESULTS

Crystal compositions

Both $RbCaF_3$ and $CsCaF_3$ crystals have the cubic perovskite structure at RT. They form $Rb_{1-x}Cs_xCaF_3$ mixed crystals for $0<x<1$ with the same RT structure. We only have found the cubic-to-tetragonal SPT in crystals with nominal compositions corresponding to x values up to 0.4. The crystals have been analyzed by atomic emission spectroscopy. The measured x values are given in Table I. From now on, we will use the x values obtained from this analysis.

X-ray diffraction measurements have also been performed at RT using powders of all the crystals. The positions of the diffraction maxima correspond to cubic crystals with a lattice parameter a changing continuously between those of the pure $RbCaF_3$ and $CsCaF_3$ samples. The a values corresponding to different compositions plotted vs x are given in Fig. 1. An approximate linear dependence of a with x is observed.

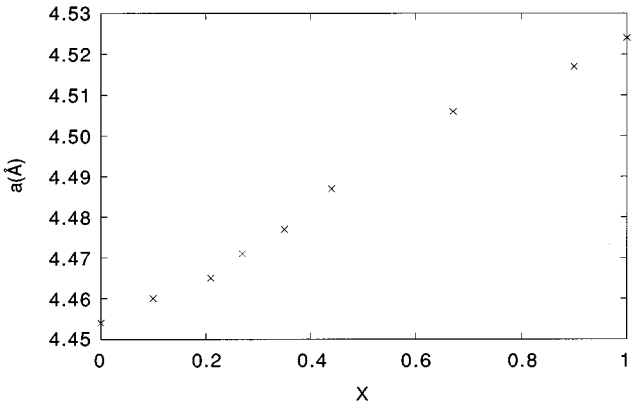

FIG. 1. Cubic lattice parameter a of the $Rb_{1-x}Cs_xCaF_3$ crystals at RT as a function of x.

Thermal expansion

The linear thermal expansion $\Delta l(T)/l_0$ has been measured on $Rb_{1-x}Cs_xCaF_3$ crystals as a function of temperature, both cooling down and warming up the sample. The results corresponding to crystals with $x \leqslant 0.44$ are shown in Fig. 2. For $x \geqslant 0.44$ no SPT's were detected. Only in pure $RbCaF_3$ the results showed thermal hysteresis (see below).

All the samples show an almost linear behavior of $[\Delta l(T)/l_0]$ vs T in the high-temperature region that corresponds to the cubic phase. At a certain temperature (the critical temperature T_c) ranging from 196 K in pure $RbCaF_3$ to 67 K in the $x=0.35$ crystals, a clear change in the slope of the $\Delta l(T)/l_0$ vs T curve is observed. The dependence of T_c with composition is shown in Fig. 3. It can be seen that T_c decreases when x increases. The change in the slope, which does not appear for $x \geqslant 0.44$, can be associated with a SPT from the cubic to the tetragonal phase similar to that reported in pure $RbCaF_3$. As we said above, this transition is second order with a small first-order component that will produce a jump in $\Delta l(T)/l_0$. This is better observed in the anomaly of the LTE coefficient $\alpha = d[\Delta l(T)/l_0]/dT$ at T_c given in Fig. 4, where the jump in $\Delta l(T)/l_0$ gives rise to a sharp peak. The sharp peak observed in the $x=0$ and $x=0.1$ samples turns broader for $x>0.1$.

The continuous change in the slope of the $\Delta l(T)/l_0$ vs T curve at $T<T_c$ is due to changes in the tetragonal distortion. In pure $RbCaF_3$, it has been found by neutron diffraction[11]

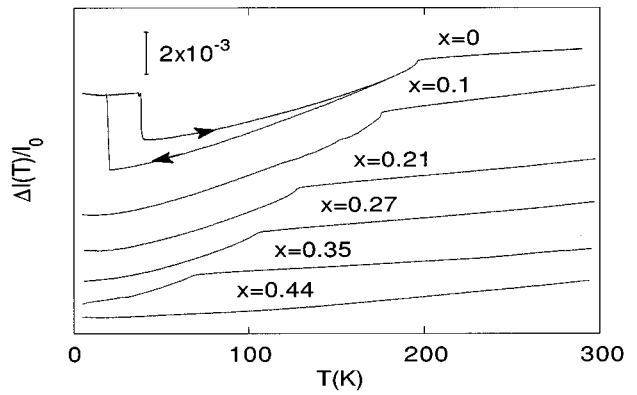

FIG. 2. Linear thermal expansion of the $Rb_{1-x}Cs_xCaF_3$ crystals with $x=0$, 0.1, 0.21, 0.27, 0.35, and 0.44.

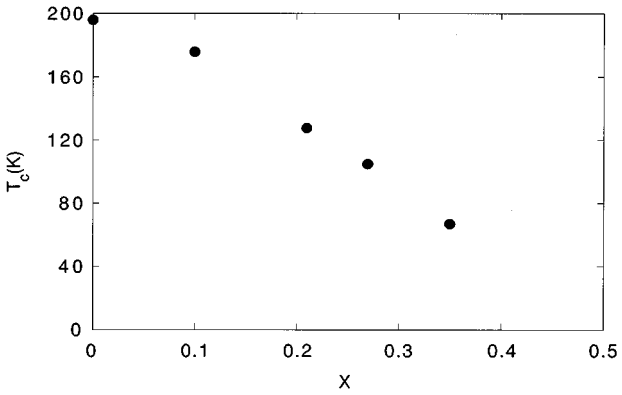

FIG. 3. Evolution of the critical temperature T_c with the crystal composition in $Rb_{1-x}Cs_xCaF_3$.

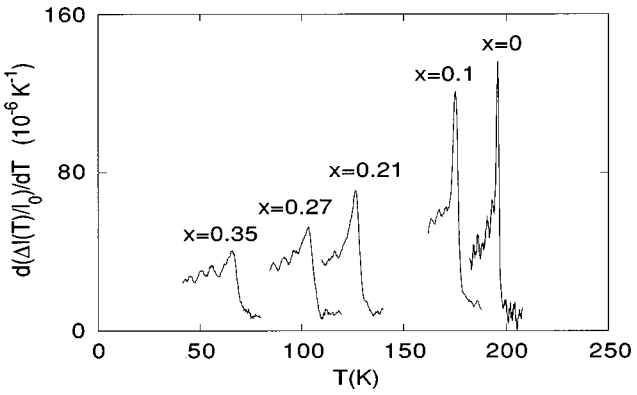

FIG. 4. Thermal dependence of the LTE coefficient, $\alpha=(d/dT)[\Delta l(T)/l_0]$, of $Rb_{1-x}Cs_xCaF_3$ crystals with $x=0$, 0.1, 0.21, 0.27, and 0.35 at temperatures close to T_c.

that the tetragonal domains expand along the direction of the tetragonal axis and are compressed in the perpendicular plane. Under these considerations, the thermal dependence of the $RbCaF_3$ curve in Fig. 2 at temperatures lower than 195 K can be related to the contributions from different domains (see below). The same explanation can be applied to the mixed crystals. From the thermal expansion data one can obtain the length of the crystal $l(T)$ as a function of temperature: $l(T)=l_0+\Delta l(T)$.

A relation between the length of the crystal and the lattice parameters can also be established. In the tetragonal phase:

$$l(T)=N[mc(T)+na(T)], \tag{1}$$

where N is the number of pseudocubic unit cells[11] in the direction of the strain gauge ([100]), $c(T)$ and $a(T)$ are the pseudocubic lattice cell parameters, respectively, as a function of T. They are related to the tetragonal cell parameters $a_t(T)$ and $c_t(T)$ by $a(T)=a_t(T)/\sqrt{2}$ and $c(T)=c_t(T)/2$. m and n are the fractions of cells with the elongated axis parallel and perpendicular, respectively, to the direction of the strain gauge. So, it must hold that

$$m+n=1. \tag{2}$$

For a random distribution of domains, $n=0.67$ and $m=0.33$, and so $n/m=2$. From crystallographic data[11] of $RbCaF_3$, it is known that, close to T_c, the elongation of the c axis is about twice the shortening of the a axis. Thus, in the case of random distribution of domains, almost no effect of the SPT on the linear thermal expansion measurements should be expected. However, the results in Fig. 2 show that the decrease of the crystal length in the tetragonal phase is faster than the linear one observed in the cubic phase. It can be concluded that we have a preferential orientation of the domains with the c axes perpendicular to the direction of the strain gauge. Since we do not know the values of the lattice parameters $a(T)$ and $c(T)$ in the mixed crystals, the ratio n/m cannot be obtained from our measurements.

In pure $RbCaF_3$, another discontinuous change in the $\Delta l(T)/l_0$ vs T curve is observed at low temperatures (see Fig. 2). The abrupt anomaly appears at about 20 K when the sample is cooled down and at 40 K during the warming up. This discontinuity is associated with the first-order SPT from the tetragonal to the orthorhombic phase and shows a thermal hysteresis of about 20 K. It can be seen that this low-temperature transition does not appear, at least at temperatures down to 10 K, in any of the mixed crystals. This can be associated with a decrease of the transition temperature when Rb^+ ions are substituted by Cs^+. It has been observed that the low-temperature SPT in $RbCaF_3$ is sample dependent and can disappear in strained samples.[11] Since more strains are expected in the mixed crystals than in the pure one, it could be argued that this might also be a reason for the disappearance of the low-temperature transition in samples with $x\neq 0$. However, in $Rb_{1-x}K_xCaF_3$ crystals this low-temperature transition has been observed with x up to 0.2.[9] Thus, we propose that, as for the cubic to tetragonal SPT, there is also a decrease of the T_c associated with the tetragonal to orthorhombic SPT when a bigger monovalent cation is substituted for a smaller one.

With respect to the thermal expansion changes in the two SPT's in pure $RbCaF_3$ (Fig. 2), it can be seen that when we cool the sample down, there is an extra contraction of the crystal at the 195 K SPT while at $T\approx 20$ K, a large increase of the length of the sample comes out. The first contraction is consistent with the model proposed for the cubic-to-tetragonal SPT if, as we have already said, the domain distribution in our samples is such that the domains with the c axis perpendicular to the strain gauge predominate in the tetragonal phase. In the low-temperature SPT, the tetragonal phase undergoes a change into an orthorhombic one which is characterized by a tilting of the cubic fluorine octahedra around the three ⟨100⟩ axes with approximately the same angle amplitude for the three rotations.[11] This is accompanied by a compression of the domains along the c axis of the tetragonal phase and an expansion in the plane perpendicular to this direction. In our crystals, because of the predominance of the domains with the c axis perpendicular to the strain gauge direction, we should get at this transition a discontinuous increase of the length along the strain gauge direction when we cool the sample down, in agreement with the experimental results.

Electron paramagnetic resonance

Ni^{2+}

The EPR spectrum of the ''as-grown'' $Rb_{1-x}Cs_xCaF_3$ crystals doped with nickel has been measured at different

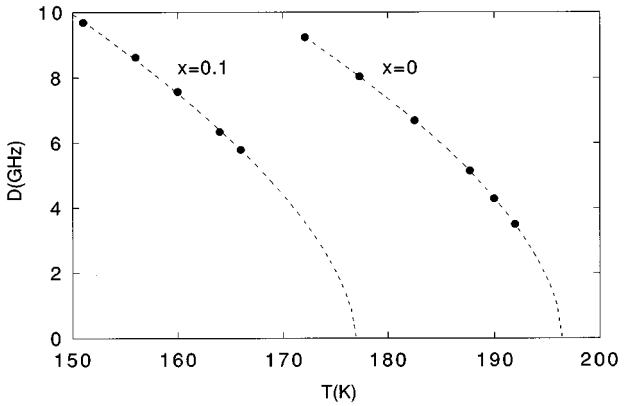

FIG. 5. Thermal dependence of the crystal field parameter D for tetragonal Ni^{2+} centers in $Rb_{1-x}Cs_xCaF_3$ crystals with $x=0$ and 0.1. Experimental values are represented by full circles. Dashed lines correspond to the best fit using Eq. (8).

temperatures and for different orientations of the static magnetic field **B**. The Ni^{2+} signal has only been detected in samples with $x=0$ and $x=0.1$. This has been associated with a strong inhomogeneous broadening of the Ni^{2+} lines. The EPR of Ni^{2+} is very sensitive to crystal field and it has linewidths of about 80 mT in pure $RbCaF_3$ due to internal stresses and inhomogeneities.[14] It can be expected that the distortions due to the mixture of Cs^+ and Rb^+ produce a strong broadening of the lines which makes them undetectable for $x>0.1$.

The thermal dependence of the Ni^{2+} EPR signal in pure $RbCaF_3$ has been previously reported.[14] Above the phase transition, the spectra correspond to Ni^{2+} ions ($S=1$) in a cubic octahedral environment. The cubic signal transforms to a tetragonal one at the critical temperature. The information about the SPT comes from the thermal dependence of this tetragonal signal. The fluorine octahedra surrounding the divalent cations are elongated in one of the $\langle 100\rangle$ directions and rotated by an angle ϕ around this direction, the rotation being alternated in neighboring octahedra. The tetragonal distortion and the angle ϕ are temperature dependent. Different domains oriented along each of the $\langle 100\rangle$ directions are usually observed. The lines positions, for different orientations of **B**, can be calculated using the following spin Hamiltonian (SH):

$$H=\mu_B B(g_\perp S_x \sin\Theta + g_\parallel S_z \cos\Theta) + D[S_z^2-(\tfrac{1}{3})S(S+1)], \tag{3}$$

with $S=1$. The z axis is along the tetragonal axis of each of the centers and Θ is the angle between the z axis and the direction of **B**. Fitting the calculated lines positions to the experimental ones measured at different temperatures, the thermal dependence of the SH parameters has been obtained. The g factors are almost temperature independent in the T range of measurement while the zero-field splitting parameter D (associated with the cubic-to-tetragonal distortion) presents a strong thermal dependence. The values of the g tensor components are $g_\parallel=2.32$ and $g_\perp=2.30$. The thermal dependence of the zero-field splitting parameter D is shown in Fig. 5.

Similar results have been obtained for the $x=0.1$ sample. In this case, the transition temperature is about 176 K in agreement with thermal expansion results. Below this temperature the Ni^{2+} signal has an overall tetragonal symmetry. The lines are broader than in the pure crystals, due to the different environments of the Ni^{2+} ions associated with the substitution of Rb^+ by Cs^+. This substitution gives place to small distortions of the tetragonal environment that do not produce a resolved splitting of the EPR signal in our spectra, but an inhomogeneous broadening. Because of this, there is a large uncertainty in the determination of the SH parameters. In particular, the small anisotropy of the g tensor in the tetragonal phase cannot be established. However, the evolution of the the signal when the applied magnetic field **B** is rotated in a {100} plane indicates that the centers have tetragonal symmetry. A fit of the line positions at different temperatures using the SH (3) considering $g_\parallel=g_\perp=g$, gives a value of $g=2.32$ as well as the thermal dependence of D shown in Fig. 5.

The Ni^{2+} EPR signal is also sensitive to the tetragonal to orthorhombic SPT. The changes observed in the spectrum below 40 K appear only in the pure crystals at the temperatures where the thermal expansion shows abrupt anomalies. A detailed study of these changes will be reported elsewhere.

Ni^{3+}

Ni^{3+} ions are produced in nickel-doped $Rb_{1-x}Cs_xCaF_3$ crystals by hole capture at Ni^{2+} during RT x irradiation. The EPR signal of Ni^{3+} can only be detected at low temperatures [below 60 K Refs. 15 and 16]. We have measured the EPR spectrum of Ni^{3+} ions in $Rb_{1-x}Cs_xCaF_3$ crystals at different temperatures and for different orientations of the static magnetic field. The results depend on the crystal composition and the temperature.

When measured at 10 K, the crystals with $x\geqslant 0.44$ show a cubic Ni^{3+} signal that is very similar to that in pure $CsCaF_3$,[15] but with broader lines. This indicates that those crystals remain in the cubic phase down to 10 K in agreement with the thermal expansion results. The lines are inhomogeneously broadened because of the existence of different environments of Ni^{3+} ions associated with the mixing of Rb^+ and Cs^+.

On the other hand, the samples with $x<0.44$ measured at 25 K show a Ni^{3+} signal with tetragonal symmetry similar to that found in pure $RbCaF_3$.[16] The lines also show a strong inhomogeneous broadening that increases with x. As a consequence, there is a large uncertainty in the experimental determination of the lines positions. These positions can be calculated for different orientations of **B** using the SH:

$$\begin{aligned} H=&\mu_B[g_\perp(S_xB_x+S_yB_y)+g_\parallel S_zB_z] \\ &+\sum_{i=1}^{2}[A_\perp(S_xI_x^i+S_yI_y^i)+A_\parallel S_zI_z^i] \\ &+\sum_{k=1}^{4}[A'_\perp(S_{x_k}I_{x_k}^k+S_{y_k}I_{y_k}^k)+A'_\parallel S_{z_k}I_{z_k}^k], \end{aligned} \tag{4}$$

where the first term corresponds to the Zeeman interaction and the second and third ones to the superhyperfine (SHF) interaction with the surrounding fluorines. In this Hamil-

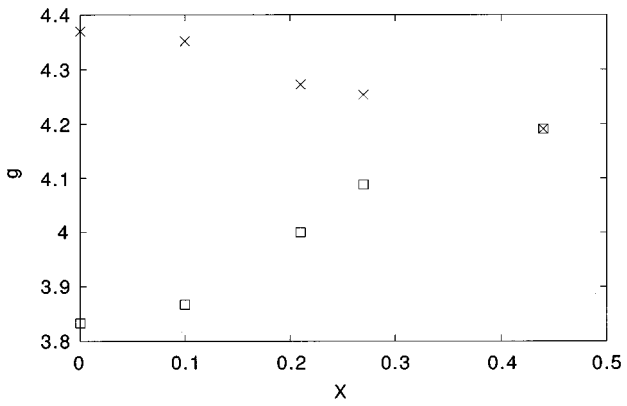

FIG. 6. Principal values of the g tensor for tetragonal Ni^{3+} centers in $Rb_{1-x}Cs_xCaF_3$ crystals with $x=0$, 0.1, 0.21, 0.27, and 0.44. × and □ represent the $g_\perp$ and $g_\parallel$ parameters, respectively.

tonian, $S=1/2$, $I=1/2$, the z axis is parallel to the tetragonal axis of the center and the z_k ones are perpendicular to that tetragonal axis and along the Ni^{3+}-F^- bonding directions (see Ref. 16).

Since the SHF splitting is only clearly resolved in the pure $RbCaF_3$ crystals, the only SH parameters that we have obtained in the mixed crystals are the principal values of the g tensor. By fitting the line positions calculated with the SH given in Eq. (4) to the experimental ones, we have obtained the results shown in Fig. 6. The anisotropy of the g tensor is due to the tetragonal distortion associated with the SPT and decreases when x increases. This indicates that the tetragonal distortion also decreases when x increases and disappears at $x=0.44$.

Finally, the Ni^{3+} EPR spectrum has been measured at 10 K with **B** along a ⟨100⟩ cubic direction. We have not found significant changes with respect to the 20 K spectra in the mixed crystals, except for the $x=0$ sample. In this case, a change from a tetragonal signal to an orthorhombic one was observed. This change is associated with the tetragonal-to-orthorhombic SPT and will be reported in detail elsewhere. All these results are consistent with those derived from LTE measurements.

DISCUSSION

The linear relationship between the x values derived from atomic emission spectroscopy and the lattice parameter measured by x-ray diffraction agrees with Vegard's law, which is usually assumed to be valid in mixed crystals.

Concerning the thermal expansion results we see that the $d[\Delta l(T)/l_0]/dT$ vs T curves given in Fig. 4 show a sharp peak at T_c for the $x=0$ and $x=0.1$ samples, while the peak is broader and rounded for $x>0.1$. It is known that the cubic-to-tetragonal SPT in pure $RbCaF_3$ is second order, but with a weak first-order component. The sharp peak in the slope of $\Delta l/l_0$ vs T in the $x=0$ sample can be associated with that first-order component. Since a similar peak appears in the $x=0.1$ sample, we conclude that the first-order component is still present in these crystals. However, in the other samples with bigger x values, the first-order character is not observed.

The same behavior has been found in some of the mixed crystals based on $KMnF_3$.[1–6] Several explanations have been given to this behavior. Borsa *et al.*[1] proposed that the rounding of the cubic-to-tetragonal SPT in $K_{1-x}Rb_xMnF_3$ crystals for $x=0.06$ is due to a distribution of transition temperatures because of fluctuations in the Rb^+ concentration. A similar explanation was given by Ratuzsna, Skrzypek and Kapusta in their study of $KMn_{1-x}Ni_xF_3$ and $KMn_{1-x}Co_xF_3$.[5] They associated the smearing out of the transition that appears for $x=0.1$ with the coexistence of two phases at $T=T_c$.

On the other hand, in an x-ray diffraction study of $KMn_{1-x}Mg_xF_3$, Cox, Giband, and Cowley[2] have found that the disappearance of the first-order character of the transition for $x=0.1$ is not accompanied by an additional broadening of the Bragg peaks which should be expected for a smeared out first-order transition. Thus they have concluded that the transition for this x value is continuous.

In our case, the broadening of the LTE coefficient for $x>0.1$ (see Fig. 4) is in favor of a smearing out of the SPT due to a distribution of transition temperatures.

Concerning the thermal evolution of the crystal length $l(T)$, the pseudocubic parameters $a(T)$ and $c(T)$ given in Ref. 11 for $RbCaF_3$ can be approximately related to the rotation angle of the fluorine octahedra ϕ by the equations

$$c(T)=a_c(T)(1+\phi^2/3),$$

$$a(T)=a_c(T)(1-\phi^2/6), \tag{5}$$

where $a_c(T)$ is the equivalent cubic cell parameter for $T<T_c$ which, for temperatures close to T_c, can be approximately obtained by extrapolation of the data of the cubic phase.

Assuming that these relations can also be applied to mixed crystals and taking into account that for a second-order transition[17] $\phi=\phi_0|T-T_0|^\beta$ (for temperatures close to T_c) we get

$$1-\frac{l(T)}{Na_c(T)}=1-\frac{l(T)}{l_c(T)}=M|T-T_0|^{2\beta}, \tag{6}$$

where M is a temperature-independent parameter related with the domain distribution, $l(T)$ is obtained from thermal expansion measurements, and $l_c(T)$ can be linearly extrapolated from the data in the cubic phase for each of the crystals.

A plot of $1-l(T)/l_c(T)$ is given in Fig. 7 for different crystal compositions. A good fit to Eq. (6) is achieved for β values close to 0.3 and for T_0 values close to T_c, in agreement with the results obtained with other techniques in $RbCaF_3$.[18] The difference in the region of $T\approx T_c$ between calculated and experimental values for the $x=0$ and $x=0.1$ samples [Fig. 7(a)] can be associated with the presence of a small first-order component in the SPT. In the other samples [Fig. 7(b)] a tail is observed in the experimental values with respect to the calculated curve. This tail can be due to the presence of different contributions to the SPT coming from regions with slightly different transition temperatures.

We will discuss now the evolution of T_c with the crystal composition (see Fig. 3). The stability of the cubic structure in AMF_3 fluororperovskites can be approximately estimated through the so-called Goldschmidt factor, which is defined as follows:

$$t=\frac{r_A+r_F}{\sqrt{2}(r_M+r_F)}, \tag{7}$$

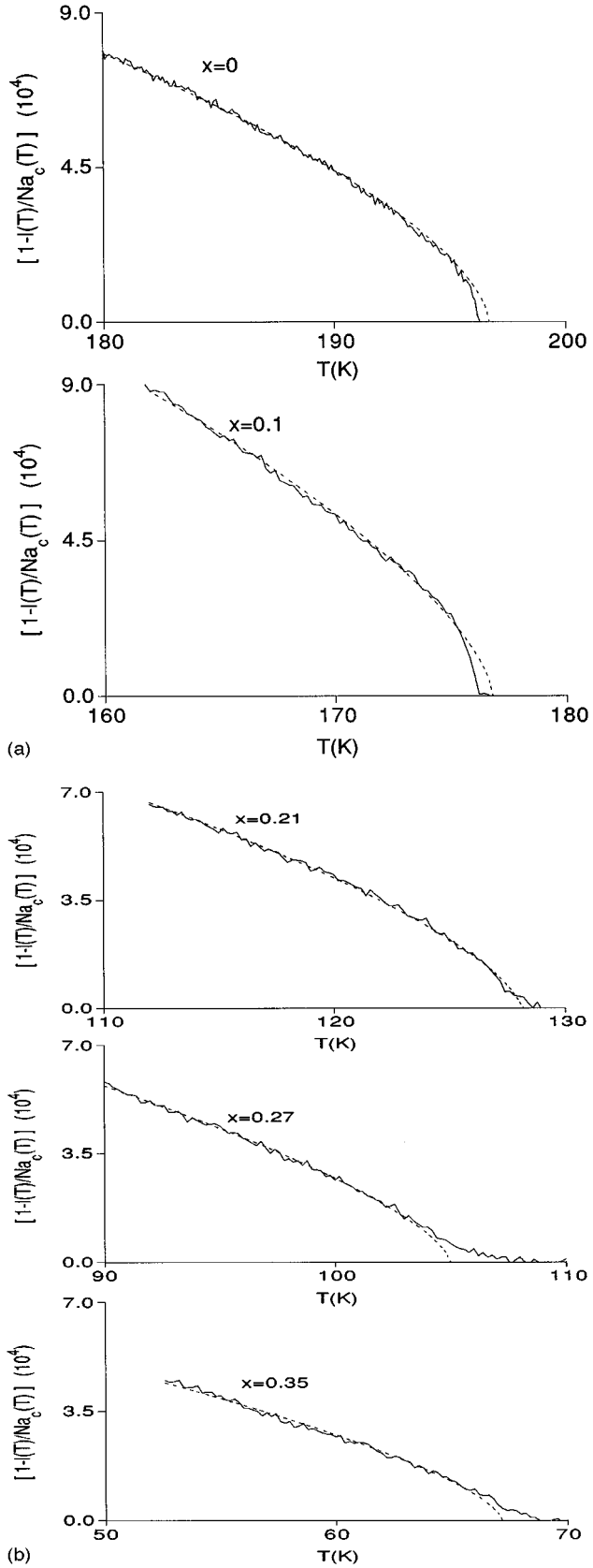

FIG. 7. $1-l(T)/\mathrm{Na}_c(T)$ vs T for $Rb_{1-x}Cs_xCaF_3$ crystals with (a) $x=0$ and $x=0.1$; and (b) $x=0.21$, 0.27, and 0.35. Solid lines represent the experimental data and dashed lines show the best fit using Eq. (6).

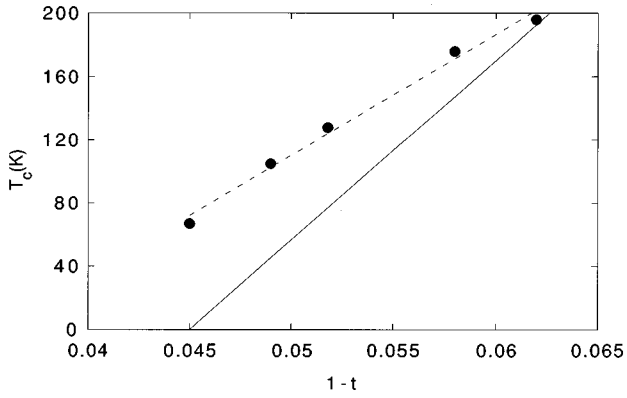

FIG. 8. Critical temperature T_c as a function of $1-t$ for $Rb_{1-x}Cs_xCaF_3$ crystals with $x=0$, 0.1, 0.21, 0.27, and 0.35. The dashed line corresponds to an approximate linear fit to our data. The continuous line is obtained from Ref. 9 (see the text).

where r_A, r_M, and r_F are the ionic radii of the corresponding ions. In the case of the mixed crystals, $Rb_{1-x}Cs_xCaF_3$, we can get an estimation of t if we consider that the radius of the monovalent cation is proportional to the mixture, i.e., $r_A=(1-x)r_{\mathrm{Rb}}+xr_{\mathrm{Cs}}$.

Working with $Rb_{1-x}K_xCaF_3$ crystals, Buzaré and co-worker[9] have found that for x values up to 0.2, there is a linear relationship between T_c and 1-t with a slope of about 1.1×10^4 K. We give in Fig. 8 a plot of T_c vs $1-t$ for our samples. The t factors have been calculated from the ionic radii given in Ref. 19 with the same considerations for the coordination number of F^- as in Ref. 9. An approximate linear behavior is found but the slope (0.9×10^4 K) is smaller than the one obtained in that reference. In Fig. 8 we show the linear dependence predicted by Buzaré and co-workers (solid line) and our approximate linear behavior (dashed line). However, when this linear behavior is extrapolated to high x values (up to 0.45), we find that the transition temperature for the $x=0.44$ sample ($1-t=0.041$) should be about 40 K, while we have not detected the transition even cooling down to 10 K. This indicates that for high x values, a faster than linear decrease of T_c vs $1-t$ appears. The same nonlinear dependence is also seen in the T_c vs x curve (Fig. 3).

This type of behavior has been observed in the SPT's of other mixed crystals (in particular in $K_{1-x}Rb_xMnF_3$ crystals that are very similar to ours) and has been explained using different models. Mitra[20] has used the model Hamiltonian formulated by Pytte and Feder[21] and Gillis and Koeler[22] to describe a second-order SPT in mixed crystals whose active atoms remain unaltered as a result of mixing. This is our situation because in $Rb_{1-x}Cs_xCaF_3$ crystals the active ions in the SPT are the fluorines.

According to Mitra, a crystal which does not have a SPT can be represented as having the critical temperature T_c either negative or infinity. If the SPT is due to a zone boundary mode, as in the cubic to tetragonal transition of $RbCaF_3$ associated with the condensation of an R mode, a negative transition temperature is related to a stronger value of the short-range interaction with respect to the long-range ones. The transition temperatures in an isomorphous crystal series where a crystal with a transition temperature T_c is diluted by

another with a negative T_c, will decrease and will vanish at a critical concentration. This is the behavior observed in our mixed crystals.

Depending on several parameters related to the interactions among the atoms which are active in the SPT and the other atoms in the crystal, Mitra has been able to predict an evolution of T_c vs x that looks very similar to ours with a faster than linear decrease of T_c when x increases. He also predicts a decrease of the order parameter with x when measured at the same temperature in all the samples. This is also in agreement with our results (see below). However, since we do not know those interaction parameters, we cannot make a quantitative calculation of the T_c vs x curve.

The β values can also be obtained from the thermal dependence of the D parameter in tetragonal Ni^{2+} centers. In our case, this can only be performed for the $x=0$ and $x=0.1$ samples that are the only ones where Ni^{2+} spectra were observed. The D values measured at different temperatures, not far from that of the phase transition Fig. 5 can be fitted to the expression

$$D(T)=D_0|T-T_0|^{2\beta}. \tag{8}$$

In a previous paper[14] on the EPR of Ni^{2+} in $RbCaF_3$ we got a β value of 0.25 taking $T_0=195$ K. Leaving D_0, T_0, and β as fitting parameters, we have obtained $\beta=0.29$ and $T_0=196.5$ K for $RbCaF_3$ and $\beta=0.30$ and $T_0=177$ K for the $x=0.1$ sample that are in good agreement with the values derived from thermal expansion data. The curves calculated with those parameters are given in Fig. 5 by dashed lines.

Finally, we will comment on the results of the EPR measurements of Ni^{3+} ions. A first conclusion is that all the samples with $x<0.44$ undergo a transition to a tetragonal phase similar to that in the pure $RbCaF_3$ crystals. The difference between parallel and perpendicular components of the g tensor is produced by the tetragonal distortion. This difference decreases when x increases, indicating that the tetragonal distortion decreases too, and has completely disappeared for $x=0.44$. The distortion is related to the order parameter, and thus our results would indicate that this order parameter, measured at 25 K decreases as x increases. This result is in agreement with Mitra's calculations[20] for mixed crystals with a T_c vs x evolution as the one given in Fig. 3.

CONCLUSIONS

$Rb_{1-x}Cs_xCaF_3$ crystals have been successfully grown by the Bridgman technique in the entire range of x concentrations. They show the cubic perovskite structure at RT. A cubic to tetragonal SPT has been observed for $x=0$, 0.1, 0.21, 0.27, and 0.35. Crystals with $x\geqslant 0.44$ remain cubic down to 10 K. Also, a tetragonal-to-orthorhombic SPT at about 20 K has also been observed in $RbCaF_3$. None of the mixed crystals experiences this second SPT, likely because of a decrease in critical temperature.

The T_c of the cubic-to-tetragonal SPT decreases when x increases. For large x values, the evolution of T_c with x deviates from the one found by Debaud-Minorel and Buzaré[9] for small mixing rates.

A weak first-order component has been observed in the cubic-to-tetragonal SPT in the $x=0$ and $x=0.1$ samples. In crystals with $x>0.1$, a smearing out of the transition is observed, which is associated with a spatial distribution of T_c in the probes.

The EPR measurements of Ni^{3+} centers at 25 K show a decrease in the tetragonality of the signal as x increases, which is related to a diminution of the tetragonal distortion in the crystal. According to Mitra's calculations[20] this is in agreement with the evolution of T_c with x.

ACKNOWLEDGMENT

This work has been supported by the CICYT (Spain) under Project No. MAT-92-1279.

[1] F. Borsa, D. J. Bernard, W. C. Walker, and A. Baviera, Phys. Rev B **15**, 84 (1977).
[2] U. J. Cox, A. Gibaud, and R. A. Cowley, Phys. Rev. Lett. **61**, 982 (1988).
[3] A. Gibaud, R. A. Cowley, and J. Nouet, Phase Trans. **14**, 129 (1989).
[4] A. Gibaud, S. M. Shapiro, J. Nouet, and H. You, Phys. Rev. B **44**, 2437 (1991).
[5] A. Ratuzsna, D. Skrzypek, and J. Kapusta, Phase Trans. **42**, 189 (1993).
[6] A. Ratuzsna, J. Phys. Condens. Matter **5**, 841 (1993).
[7] J. Y. Buzaré and P. Foucher, J. Phys. Condens. Matter **3**, 2535 (1991).
[8] A. M. Minorel, G. Silly, and J. Y. Buzaré, Ferroelectrics **124**, 297 (1991).
[9] A. M. Debaud-Minorel and J. Y. Buzaré, J. Phys. Condens. Matter **6**, 2189 (1994).
[10] F. A. Modine, E. Sonder, W. P. Unruh, C. B. Finch, and R. D. Westbrook, Phys. Rev. B **10**, 1623 (1974).
[11] A. Bulou, C. Ridou, M. Rousseau, J. Nouet, and A. W. Hewat, J. Phys. (Paris) **41**, 87 (1980).
[12] A. Kassan-Ogly and V. E. Naish, Acta Crystallogr. Sect. B **42**, 287 (1986).
[13] A. Ratuszna and A. Kachel, Acta Crystallogr. Sect. B **48**, 118 (1992).
[14] B. Villacampa, R. Alcalá, P. J. Alonso, and J. M. Spaeth, J. Phys. Condens. Matter **5**, 747 (1993).
[15] R. Alcalá and B. Villacampa, Solid State Commun. **90**, 13 (1993).
[16] R. Alcalá, E. Zorita, P. J. Alonso, T. Hangleiter, and J. M. Spaeth, Solid State Commun. **68**, 167 (1988).
[17] M. E. Lines and A. M. Glass, *Principles and Applications of Ferroelectrics and Related Materials* (Clarendon, Oxford, 1979).
[18] H. Jex, J. Maetz, and M. Müllner. Phys. Rev. B **21**, 1209 (1980).
[19] R. D. Shanon, Acta Crystallogr. Sect. A **32**, 751 (1976).
[20] S. S. Mitra, J. Phys. C **15**, 453 (1982).
[21] E. Pytte and J. Feder, Phys. Rev. **187**, 1077 (1969).
[22] N. S. Gillis and T. R. Koehler, Phys. Rev. B **7**, 4980 (1973).